How Thick is a Fault? Fault Displacement-Thickness Scaling Revisited.

Zoe K. Shipton, Aisling M. Soden, James D. Kirkpatrick

Department of Geographical and Earth Sciences, University of Glasgow, Glasgow Scotland

Aileen M. Bright

Department of Geology, Trinity College, Dublin, Ireland

Rebecca J. Lunn

Department of Civil Engineering, University of Strathclyde, Glasgow, Scotland

Fault zone thickness is an important parameter for many seismological models. We present three new fault thickness datasets from different tectonic settings and host rock types. Individual fault zone components (i.e., principal slip zones, fault core, damage zone) display distinct displacement-thickness scaling relationships. Fault component thickness is dependent on the type of deformation elements (e.g., open fractures, gouge, breccia) that accommodate strain, the host lithology, and the geometry of pre-existing structures. A compilation of published fault displacement-thickness data shows a positive trend over seven orders of magnitude, but with three orders of magnitude scatter at a single displacement value. Rather than applying a single power-law scaling relationship to all fault thickness data, it is more appropriate and useful to seek separate scaling relationships for each fault zone component and to understand the controls on such scaling.

INTRODUCTION

Faults are generally composed of three components: one or more principal slip zones (PSZ, also referred to as principal displacement zones or principal slip surfaces) sitting within a fault core (FC) where most of the displacement is accommodated, surrounded by an associated zone of fractures known as the damage zone (DZ) [*Caine et al.*, 1996; *Schulz and Evans*, 1998; *Chester et al.*, 2004]. Although some co-seismic slip may occur within the DZ it is likely that the majority of earthquake slip occurs within the FC and PSZ. Many processes that may explain the dynamic reduction of shear resistance during earthquakes require that the zone that slips during an earthquake has a specific thickness. Elastohydrodynamic fault lubrication could occur between surfaces less than 1 to 5 mm apart [*Brodsky and Kanamori*, 2001]. Frictional melting and transient thermal pressurization of fluids requires that the PSZ is less than centimeters in thickness [*Bizzarri and Cocco*, 2006; *Wibberley and Shimamoto*, 2005]. Conversely the acoustic fluidization model of *Melosh* [1996] requires fluidization of a zone 1 to 20 m thick. Damage zone thickness will constrain the magnitude of potential energy sinks due to creation of new fractures or slip along existing fractures around a dynamically slipping fault [*Poliakov et al.*, 2002; *Dalguer et al.*, 2003; *Andrews*, 2005]. Geophysical data also image different parts of the PSZ/FC/DZ system. Anomalous low resistivity zones up to 1 km thick across the San Andreas fault are attributed to fluid-filled fractures in the DZ [*Unsworth et al.*, 1999]. Conversely, co-location of aftershocks [*McGuire and Ben-Zion*, 2005] and microearthquake distribution [*Nadeau and McEvilly*, 1997] shows that the region that slips during an earthquake (the PSZ) may be as narrow as 1-5 m.

In this paper we present three new displacement-thickness datasets, from fault populations in three different lithologies. Fault core and DZ thickness have been measured at points where true displacement can be calculated from slip vector orientations and the separation of markers across the fault. We distinguish here between *displacement* measured on an exhumed fault and the *slip* that occurs in an earthquake that ruptures along a fault. Fault zone components are distinguished on the basis of the type of deformation ele-

ments that they contain (structures within the fault such as gouge, fractures, breccia, deformation bands) and the spatial distribution and density of those deformation elements. We compare our data to a compilation of fault "thickness" data from previous studies of faults in a wide range of host rock types and tectonic settings. Although a correlation apparently exists between thickness and displacement, we argue that a single power law relationship is not appropriate, and is not useful for describing or predicting fault zone thicknesses. Distinct thickness-displacement relationships can arise depending on the deformation elements dominant in different lithologies, at different times in the development of a single fault, and under different deformation conditions.

SHALLOW NORMAL FAULTS IN SANDSTONE

Faults in sandstone with porosity greater than 10% are dominated by deformation elements called deformation bands [see review in *Schultz and Siddharthan*, 2005]. Deformation bands are mm-thick tabular zones of grain crushing with mm of displacement. Increased displacement is accommodated by the addition of more bands to a zone until a slip-surface nucleates. Once nucleated, slip-surfaces propagate, often along the edges of zones of bands, to form a through-going slip-surface (PSZ) which can accommodate meters to kilometers of total displacement.

The Big Hole normal fault in central Utah developed in the 20-24% porosity Navajo Sandstone at overburden depths of 1.5 to 3.0 km [*Shipton and Cowie*, 2001]. The fault core consists of amalgamated deformation bands and occasional breccias. At any point on the fault the FC thickness varies by an order of magnitude (Figure 1), but it tends to be thicker at areas of fault linkage [*Shipton and Cowie*, 2001]. The DZ surrounding the FC consists of deformation bands with occasional short segments of slip-surfaces [*Shipton and Cowie*, 2001]. There is a positive correlation between DZ thickness and displacement, but there is no change in the mean thickness of the fault core as fault displacement increases (Figure 1).

FIGURE 1

REACTIVATED NORMAL FAULTS IN IGNIMBRITES

Cycles of eruption on the volcanic island of Gran Canaria deposited numerous ignimbrite flows across active normal fault scarps [*Troll et al*., 2002]. Ignimbrites are deposited from flows of hot ash, crystals and pumice fragments and are classified by the degree of welding (intensity of compaction and fusion that occurs during deposition). More welded ignimbrites are denser and have lower porosity. Data in Figure 2 are from normal growth faults that cut several ignimbrites with different mineralogies and degrees of welding. Only one of the studied faults contains a recognizable PSZ. In the remaining faults, deformation is distributed within the FC. The deformation elements in the FC are gouge and/or breccia. In high- to moderately-welded ignimbrites, the DZ is defined by intense jointing, with joint density decreasing away from the FC. In poorly welded ignimbrites the damage zone contains deformation bands.

The FC thickness is dependent on joint spacing in the DZ: wide fault cores coincide with widely spaced joints regardless of displacement. Damage zone joint density is controlled by two main factors. Thin ignimbrites have closer spaced joints than thicker ignimbrites so each ignimbrite may be acting as a mechanical layer that controls joint spacing [see *Bai and Pollard* 2000]. Ignimbrites with a lower proportion of pumice clasts and pores, tend to have DZs containing fewer joints. *Moon* [1993] and *Wilson et al*. [2003] suggest that the size, proportion and elastic moduli of heterogeneities such as pumice clasts and pore spaces influence stress concentrations and therefore joint density.

FIGURE 2

STRIKE-SLIP FAULTS IN GRANITES FROM SEISMOGENIC DEPTHS

Strike-slip faults cut granodiorite at many localities in the central Sierra Nevada, California. Isotopic dating of micas formed in fault gouge coupled with amphibole geobarometry suggests that some of the faults in the area were active near the base of the seismogenic zone [*Pachell and Evans*, 2002]. Faults in the Mount Abbot area nucleated on pre-existing cooling joints [*Segall and Pollard*, 1983]. Single reactivated joints linked, through dilational splay fractures developed at their tips, into mature 'compound fault zones' [*Martel*, 1990]. Compound fault zones are defined by two parallel fault cores bounding a zone of highly fractured host rock. In the Granite Pass area (*Evans et al.* 2000) some of the faults developed according to *Martel's* [1990] model, but others have a FC defined by a single zone of cataclasite and ultra-

cataclasite. The damage zone of both fault styles consists of open mode fractures and minor faults, especially around points where large faults linked (see Figures 4 and 5 in *Evans et al.,* 2000).

For reactivated joints not linked to other small faults, the FC is defined by a narrow, mineral-filled sheared joint. The thickness of these sheared joints does not change with displacements up to 1m (Figure 3). For larger faults with single cataclasite FCs, the thickness increases with displacement. For compound fault zones, both the total thickness of the two bounding faults, and the distance between the bounding faults, increases with displacement.

FIGURE 3

DISCUSSION AND CONCLUSIONS

The existence of a scaling relationship between thickness and displacement would allow predictions to be made of the thickness of fault zones at seismogenic depths. *Robertson* [1983], *Scholz* [1987] and *Hull* [1988] suggested that a linear scaling relationship exists between fault thickness and displacement. However *Blenkinsop* [1989] and *Evans* [1990] argued that this relationship was spurious as it included fault thickness data from many fault populations in a wide range of rock types. These authors also stress that the data presented by *Scholz* [1987] and *Hull* [1988] often did not explicitly state how the net displacement was determined and in what direction thickness was measured relative to the slip vector.

The type of deformation elements present in a fault zone is highly dependent on the lithology being deformed and the pressure, temperature and strain rate during deformation. There are no standard criteria to define fault components across all fault zones, because the definition of FC and DZ depends on the deformation elements that occur within the fault zone. This leads to a degree of subjectivity in the definition of the boundaries of the fault core and damage zone. In fact, *Schultz and Evans* [1998, their figure 16] showed that the width of a single fault's DZ can vary by an order of magnitude depending on which deformation elements are used to define the DZ. Furthermore, the DZ is often asymmetric around the FC and PSZ [e.g., *Shipton and Cowie,* 2001; *Heermance et al.,* 2003; *Dor et al.,* 2005]. The dominant deformation elements within each part of the fault zone may also change over time, for instance due to varying stress conditions [*Knipe and Lloyd,* 1994] or rock rheology [*Johansen et al*., 2005]. *Power et al.* [1988] suggested that smoothing of rough surfaces as displacement accumulated could lead to a steady state FC thickness. However a fault with self-similar roughness samples asperities with larger amplitudes as displacement increases, so real faults may not reach a steady-state thickness [*Power et al*., 1988].

Often the FC contains distinct deformation elements from the DZ. For instance, the DZ of faults in high porosity sandstones typically contain deformation bands with subsidiary slip surfaces, whereas the FC is characterized by a through-going slip surface surrounded by amalgamated deformation bands, gouge and breccia. *Shipton and Cowie* [2003] suggest that bulk strain hardening results in an increase of DZ thickness as the number of displacement events at a point on the fault increases. Conversely, the FC is dominated by linkage of DZ faults with the main FC resulting in a highly heterogeneous FC thickness along strike, which has no simple relationship with displacement.

Different lithologies may deform with different deformation elements under the same stress state, strain rate etc. In the dataset presented in Figure 2, ignimbrite lithology and fabric exert a strong control on DZ thickness. In heterogeneous moderately-welded (unit A) to highly-welded (unit B) ignimbrites the FC is formed when slabs between joints are rotated and broken down to form breccia and gouge. Joint spacing will therefore control the width of the slabs and ultimately the amount of wear material formed in the FC. In these heterogeneous units, the thickness of the joint-dominated DZ decreases with displacement. However these units have only a weak increase of FC thickness with displacement. The more homogeneous unit (unit X) permits more bulk deformation at the grain scale, limiting joint formation and therefore the extent of the FC and DZ.

The geometry of pre-existing structures also exerts a strong control on fault geometry. The Sierra Nevada faults nucleated on pre-existing joints, and FC thickness for the small faults (<1m displacement) is controlled by the width of the pre-existing opening mode fractures. Once the faults start to link up to form larger fault zones, more material is progressively included into the FC, resulting in a positive scaling of thickness and displacement. The change in deformation process from joint reactivation in the small faults, to linkage of reactivated joints and cataclasis in the large faults, produces a corresponding change in the scaling of FC thickness and displacement.

Given the dependence of fault thickness on so many interrelated factors, we suggest that a single displacement-thickness correlation is not appropriate for mak-

ing predictions about fault zone properties. Figure 4 shows a compilation of fault displacement-thickness data from sixteen fault populations, including data from *Scholz* [1987] and *Hull* [1988]. The thickness-displacement dataset in Figure 4 is available in the CD-ROM attached to this volume. Although an overall positive trend can be observed over seven orders of magnitude, there is more than three orders of magnitude scatter at any value of displacement. The relationships for individual datasets are often not well described by the best fit line to the overall trend. Towards the top of Figure 4, two DZ datasets from sandstone are clearly not well predicted by the best fit line, which would predict DZ thicknesses in sandstone at small displacements (10cm or less) at least four orders of magnitude too small. Three relationships for granite are also shown on Figure 4. Whilst the individual datasets are not too far from the overall trend line, their gradients vary significantly. Consequently, predictions based on the site-specific fault thickness data for a displacement of ~10m would vary by at least two orders of magnitude, with only the pseudotachylyte prediction being close to the overall trend line.

FIGURE 4

Although many of the fault datasets in Figure 4 are not from unequivocally seismogenic faults [i.e., do not host pseudotachylytes, see *Cowan* 1999], this compilation is still useful to show that *global* fault zone thickness correlations should not be used to understand earthquake processes. Different fault zone components will host different active processes during an earthquake event. The thickness of zone of active slip during an earthquake (the PSZ and perhaps the FC) will have important controls on slip-weakening mechanisms and energy loss on the slip plane. The thickness of the damage zone may affect the magnitude of the energy sink that the damage zone provides and control the rupture propagation along the fault surface. Future field studies should explicitly state which deformation elements are used to define the principal slip zone, fault core and damage zone, and to measure the thickness of each of these independently. It would be highly valuable to undertake studies of the controls on fault thickness within seismogenic faults that have developed by specific faulting processes, and under different deformation conditions. Fault structures from exhumed outcrops will contain deformation elements created during seismic slip but also during the interseismic period [*Cowan,* 1999], both of which will contribute to the final displacement on an exhumed fault. Further studies are needed to recognize features which might allow us, in the absence of pseudotachylytes, to distinguish which parts of a fault zone were formed during seismic ruptures and which were produced aseismically.

Acknowledgments. Fabrizio Storti, Rick Sibson and Giulio Di Toro gave constructive reviews of this paper. AMS and JDK are supported by University of Glasgow graduate scholarships; AMB was supported by Enterprise Ireland grant SC/02/261 Thanks to the US National Park Service and the USDA Forest Service for permission to work in the Sierra Nevada, to Valentin Troll for guidance on Gran Canaria, and Jim Evans, Tom Blenkinsop, Emily Brodsky and Rachel Abercrombie for valuable discussions.

REFERENCES

Andrews D. J. (2005), Rupture dynamics with energy loss outside the slip zone, *J. Geophys. Res., 110*, B01307, doi:10.1029/2004JB003191.

Bai, T. and D. D. Pollard (2000), Closely spaced fractures in layered rocks: initiation mechanism and propagation kinematics, *J. Struct. Geol., 22*, 1409-1425.

Blenkinsop, T. B. (1989), Thickness-displacement relationships for deformation zones: Discussion, *J. Struct. Geol., 11*, 1051-1054.

Bizzarri, A., and M. Cocco (2006), A thermal pressurization model for the spontaneous dynamic rupture propagation on a three-dimensional fault: 1. Methodological approach, *J. Geophys. Res., 111*, B05303, doi:10.1029/2005JB003862.

Caine, J. S., J. P. Evans, and C. B. Forster (1996), Fault zone architecture and permeability structure, *Geology, 24*, 1025-1028.

Chester, F. M., J. S. Chester, D. L. Kirschner, S. E. Schulz, and J. P. Evans (2004), Structure of large-displacement strike-slip fault zones in the brittle continental crust. In: *Rheology and Deformation in the Lithosphere at Continental Margins*, edited by Karner, G. D., B. Taylor, N. W. Driscoll, and D. L. Kohlstedt, Columbia University Press, New York.

Dalguer L. A., K. Irikura, and J. D. Riera (2003), Simulation of tensile crack generation by three-dimensional dynamic shear rupture propagation during an earthquake, *J. Geophys. Res., 108*(B3), 2144, doi:10.1029/2001JB001738.

Dor O., T. K. Rockwell and Y. Ben-Zion, (2006), Geologic observations of damage asymmetry in the structure of the San Jacinto, San Andreas and Punchbowl faults in southern California: A possible indicator for preferred rupture propagation direction, *Pure Appl. Geophys., 163*, 301-349, DOI 10.1007/s00024-005-0023-9.

Evans, J. P. (1990), Thickness-displacement relationships for fault zones, *J. Struct. Geol., 12*, 1061-1065.

Evans, J. P., Z. K. Shipton, M. A. Pachell, S. J. Lim and K. Robeson (2000), The structure and composition of exhumed faults, and their implications for seismic processes. In: *Proc. 3rd Conf. on Tectonic Problems of the San Andreas Fault System*. Bokelmann, G. and Kovach, R.L. (eds.) Stanford University Publications, Geological Sciences 21, 67-81.

Heermance, R., Z. K. Shipton, and J. P. Evans (2003), Fault structure control on fault slip and ground motion during the 1999 rupture of the Chelungpu fault, Taiwan, *Bull. Seis.l Soc. Am.*, *93*, 1034-1050.

Hull, J. (1988), Thickness-displacement relationships for deformation zones, *J. Struct. Geol., 10*, 431-435.

Johansen, T. E. S., H. Fossen, and R. Kluge (2005), The impact of syn-faulting porosity reduction on damage zone architecture in porous sandstone: an outcrop example from the Moab Fault, Utah, *J. Struct. Geol., 27*, 1469-1485.

Knipe, R. J., and G. E. Lloyd (1994), Microstructural analysis of faulting in quartzite, Assynt, NW Scotland: Implications for fault zone evolution, *Pure Appl. Geophys., 143*, 229-254.

Martel, S. J. (1990), Formation of Compound Strike-Slip-Fault Zones, Mount Abbot Quadrangle, California, *J. Struct. Geol., 12*, 869.

Melosh H. J. (1996), Dynamical weakening of faults by acoustic fluidization, *Nature, 379*, 601 – 606.

McGuire, J., and Y. Ben-Zion (2005), High-resolution imaging of the Bear Valley section of the San Andreas fault at seismogenic depths with fault-zone head waves and relocated seismicity, *Geophys. J. Int., 163*, 152–164.

Moon, V. G. (1993), Geotechnical characteristics of ignimbrite: A soft pyroclastic rock type, *Eng. Geol., 35*, 33-45.

Nadeau, R. M., and T. V. McEvilly (1997), Seismic studies at Parkfield; V, Characteristic microearthquake sequences as fault-zone drilling targets, *Bull. Seis Soc Am., 87*, 1463-1472

Pachell, M. A., and J. P. Evans (2002), Growth, linkage, and termination processes of a 10-km-long strike-slip fault in jointed granite: the Gemini fault zone, Sierra Nevada, California, *J. Struct. Geol., 24*, 1903-1924.

Poliakov, A. N. B., R. Dmowska, and J. R. Rice (2002), Dynamic shear rupture interactions with fault bends and off-axis secondary faulting, *J. Geophys. Res., 107* (B11), 2295, doi:10.1029/2001JB000572.

Power, W. L., T. E. Tullis, and J. D. Weeks (1988), Roughness and wear during brittle faulting, *J. Geophys. Res., 98* (B12), 15268-15278.

Robertson, E. C. (1983), Relationship of fault displacement to gouge and breccia thickness, *American Institute of Mining Engineers Transactions, 274*, 1426-1432.

Scholz, C. H. (1987), Wear and gouge formation in brittle faulting, *Geology, 15*, 493-495.

Schulz, S. E., and J. P. Evans (1998), Spatial variability in microscopic deformation and composition of the Punchbowl fault, southern California: implications for mechanisms, fluid-rock interaction, and fault morphology, *Tectonophys., 295*, 223-244.

Schultz, R. A. and R. Siddharthan (2005), A general framework for the occurrence and faulting of deformation bands in porous granular rocks. *Tectonophys., 411*, 1-18.

Segall, P., and D. D. Pollard (1983), Nucleation and Growth of Strike Slip Faults in Granite, *J. Geophys. Res., 88*, 555-568.

Shipton Z. K. and P. A. Cowie (2001), Damage zone and slip-surface evolution over μm to km scales in high-porosity Navajo sandstone, Utah, *J. Struct. Geol., 23*, 1825-1844.

Shipton, Z. K., and P. A. Cowie (2003), A conceptual model for the origin of fault damage zone structures in high-porosity sandstone, *J. Struct. Geol., 25*, 333-345.

Sibson, R. H. (2003), Thickness of the seismic slip zone, *Bull. Seis. Soc. Am, 93*, 1169-1178.

Troll, V. R., T. R. Walter, and H.-U. Schmincke (2002), Cyclic caldera collapse: Piston or piecemeal subsidence? Field and experimental evidence, *Geology, 30*, 135-138.

Unsworth, M, G. Egbert, and J. Booker (1999), High-resolution electromagnetic imaging of the San Andreas fault in central California, *J. Geophys. Res., 104* (B1), 1131-1150, 10.1029/98JB01755.

Wibberley, C. A. J. and T. Shimamoto (2005) Earthquake slip weakening and asperities explained by thermal pressurization, *Nature 436* doi:10.1038/nature03901

Wilson, J. E., L. B. Goodwin, and C. J. Lewis (2003), Deformation bands in non-welded ignimbrites: Petrophysical controls on fault-zone deformation and evidence of preferential fluid flow, *Geology, 31*, 837-840.

Aileen M. Bright, Department of Geology, Trinity College, Dublin 2, Ireland

James D. Kirkpatrick, Zoe K. Shipton*, Aisling M. Soden, Department of Geographical and Earth Sciences, University of Glasgow, Glasgow G12 8QQ, Scotland * zoe.shipton@ges.gla.ac.uk

Rebecca J. Lunn, Department of Civil Engineering, University of Strathclyde, Glasgow, G4 ONG, Scotland.

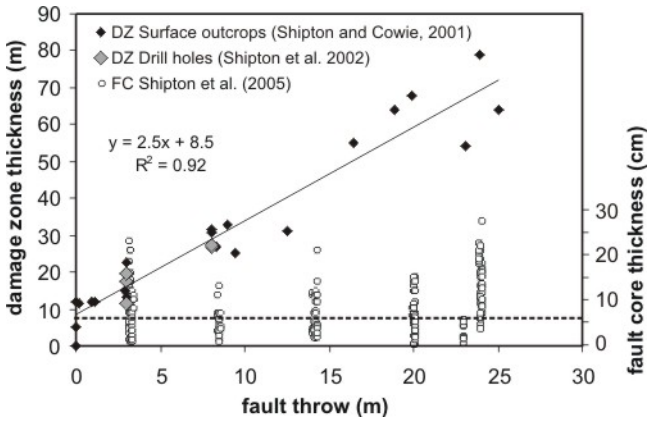

Figure 1. Damage zone and fault core thickness for the Big Hole normal fault, Utah, plotted against the vertical displacement (fault throw) of the top of the Navajo Sandstone. The horizontal damage zone thickness is measured from an envelope that surrounds all the damage zone deformation elements. The solid line shows a linear regression through the damage zone thickness data. Fault core thickness measurements were taken every 30 cm along six 10 to 25 m-long transects along the PSZ. Note that there is an order of magnitude scatter in thickness at each of the six locations. The dotted line shows the mean fault core thickness (6 cm) for all the locations.

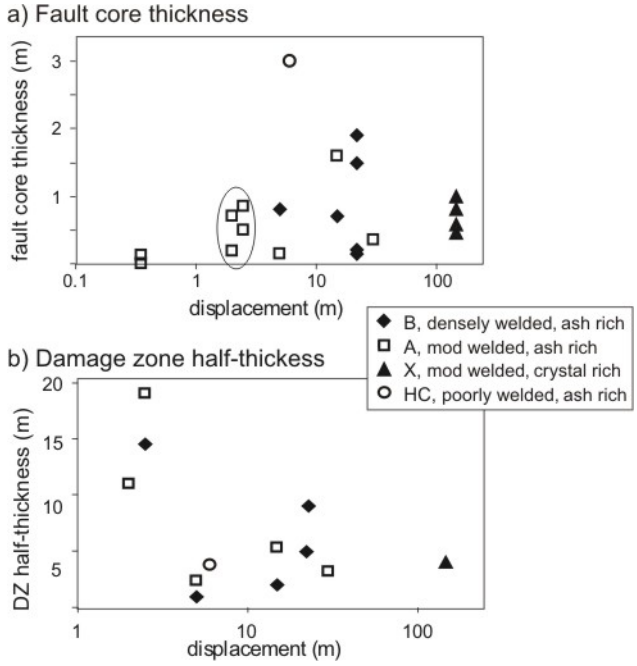

Figure 2. Log-normal plots of a) fault core thickness and b) damage zone half-width against displacement for normal faults cutting ignimbrite units of varying composition from Gran Canaria, Spain. Fault core and damage zone thickness were measured from cross-sections through a number of normal fault zones with displacement values defined by the separation of ignimbrite packages. At many sites the faults juxtapose different ignimbrite units so only half of the DZ thickness can be measured (from the FC to one edge of the DZ). However, the full thickness of the FC is measured at each location. The measurements circled in a) are taken from locations 1.5m apart along the same fault, which shows that the FC thickness changes significantly down-dip over short distances.

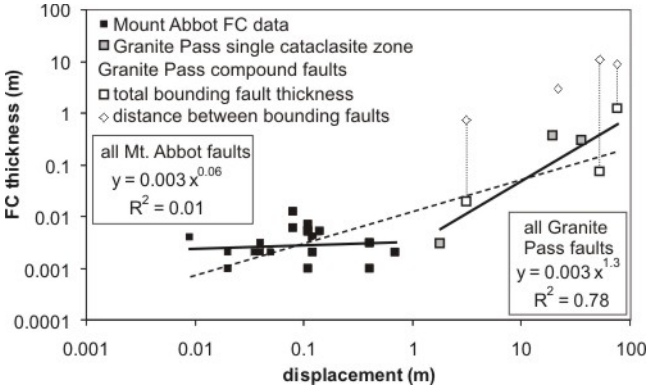

Figure 3. Log-log plot of fault core thickness against displacement from the Sierra Nevada, California showing two distinct trends. Strike-slip displacement was defined by the separation of dykes. Faults with displacement <1m from the Mount Abbot area show that thickness does not increase with displacement. Thickness increases with displacement for longer faults in the Granite Pass area where some of the faults are compound fault zones in the sense of *Martel* [1990] (open symbols) and some of the faults have a single cataclasite and ultra-cataclasite FC (grey squares). For compound fault zones, diamonds show the distance between the bounding faults and squares show the total thickness of the two bounding faults. Vertical lines connect data collected from the same fault. Note that a single power-law for this dataset (dashed line) would underestimate thickness for faults

with displacement <10 cm and >10 m.

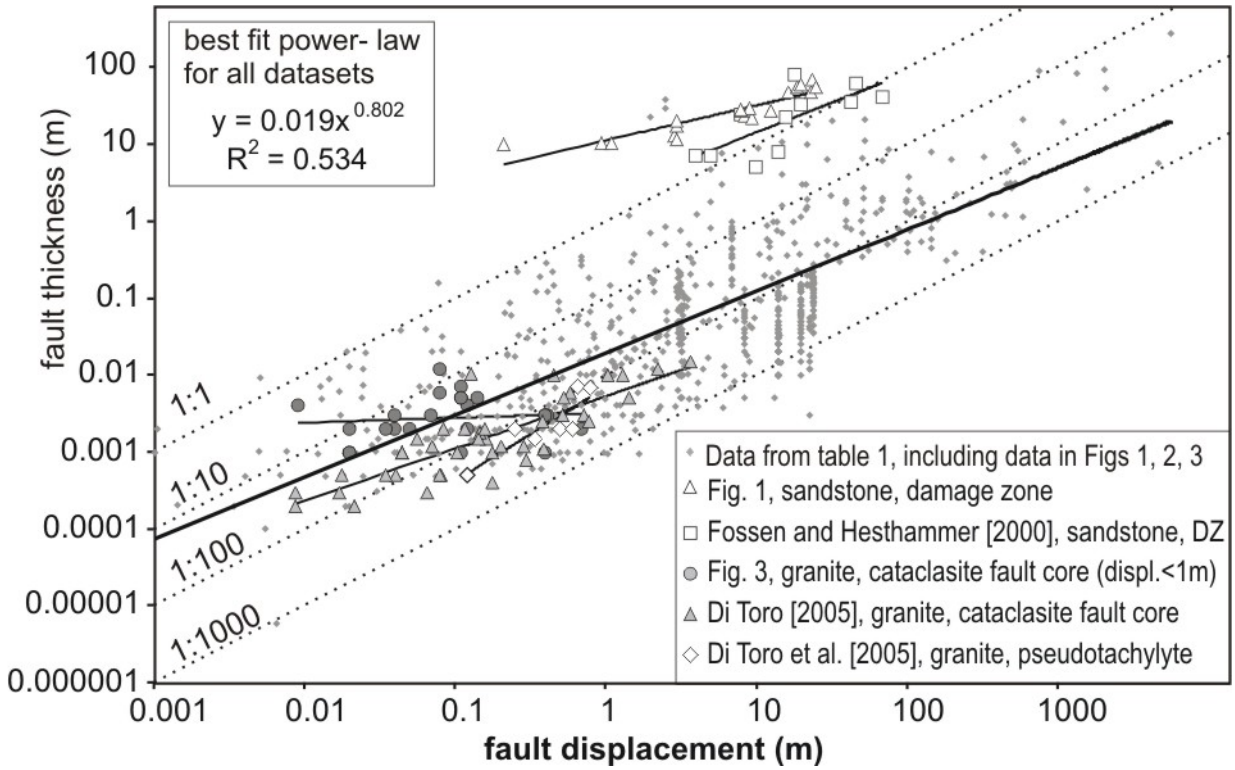

Figure 4. Log-log plot of a compilation of 16 fault thickness datasets reported in the literature including the data used by *Hull* [1988], and the three datasets in this paper. In many reported datasets no distinction is made between FC and DZ thickness. Five individual datasets are highlighted with their best-fit power laws to emphasize that the trend for the global dataset rarely describes that for individual datasets. Table 1 is available in the CD-ROM attached to this volume.

Electronic annex to *How Thick is a Fault? Fault Displacement-Thickness Scaling Revisited*. Zoe K. Shipton, Aisling M. Soden, James D. Kirkpatrick, Aileen M. Bright and Rebecca J. Lunn

Table 1. Summary of data presented in Figure 4. For each dataset we define the host rock lithology and the definition of thickness that is reported. Criteria for distinguishing fault core and damage zone width are not always well-defined in these papers, but we have attempted to classify each dataset by whether it contains mainly fault core or mainly damage zone. If it unclear, we have defined a dataset as fault zone. Some workers exclude blocks of host rock that have been entrained in the fault core (no host rock). For each of the datasets we give the exponent, coefficient and regression coefficient of the best-fitting power law. The reader is referred to the original papers for details of the datasets. Data used in the compilations of Hull [1988] and Scholz [1987] are starred.

Source	**Host lithology +/- fault type**	**measurement**	**#**	**exponent**	**coefficient**	**R^2**
Figure 1, deformation band faults	Sandstone, normal fault	Fault core	269	0.247	0.027	0.047
Figure 1, deformation band faults	Sandstone, normal fault	Damage zone	19	0.454	11.07	0.824
Figure 2, joint-dominated faults	Ignimbrites, normal growth fault	Fault core	20	0.331	0.209	0.231
Figure 2, joint-dominated faults	Ignimbrites, normal growth fault	Damage zone	12	-0.211	15.57	0.092
Figure 3, Mount Abbot, sheared joints	Granite, strike-slip fault, (<1m slip)	Fault core	23	0.063	0.003	0.012
Figure 3, Granite Pass, faults with single fault core	Granite, strike-slip fault, (>1m slip)	Fault core	3	0.002	1.657	0.947
Figure 3, Granite Pass, compound faults	Granite, strike-slip fault , (>1m slip)	Total fault core thickness	3	0.006	0.999	0.654
Di Toro and Pennacchioni, 2005; Di Toro et al, 2005	Pseudotachylyte and cataclasite in Tonalites, strike-slip fault	Slip zone	46	0.791	0.024	0.729
Sibson 1975	Pseudotachylyte in Gneiss (separations), thrust	Slip zone	14	0.519	0.140	0.898
Fossen & Hesthammer, 2000	Sandstones	Damage zone	11	0.766	2.410	0.530
Knott, 1994	Sandstones, normal (reactivated)	Damage zone	42	0.443	0.175	0.438
*Otsuki, 1978	Silt	Damage zone	6	0.409	0.040	0.506
*Otsuki, 1978	Semi-consolidated sand	Damage zone	11	0.531	0.095	0.691

Foxford et al., 1998	Sandstone & mudstone, normal	Fault core	19	0.332	0.238	0.304
Knott et al., 1996	Shale/Shale, no host rock, normal	Fault core	22	0.545	0.036	0.434
Knott et al., 1996	Sandstone/Shale, no host rock, normal	Fault core	47	0.811	0.016	0.682
Knott et al, 1996	Sandstone/sandstone, no host rock, normal	Fault core	57	0.768	0.054	0.739
Little, 1995	Mudstns, congls and ssts “Black gouge”, strike-slip fault	Fault core	13	0.445	0.003	0.720
Little, 1995	Mudstns, congls and ssts “Grey gouge”, strike-slip fault	Fault core	15	1.008	0.018	0.537
Marrett & Almendinger, 1990	“Red beds” NW Argentina “Gouge”, thrust	Fault core	23	0.743	0.014	0.722
Marrett & Almendinger, 1990	Qda Carachi “Gouge”, thrust	Fault core	23	1.004	0.012	0.982
*Robertson, 1983	Quartz monzonite “Gouge zone”	Fault core	36	0.961	0.014	0.851
*Segall & Pollard, 1983; Segall & Simpson, 1986	Granite, strike-slip fault	Fault core	7	0.563	0.120	0.319

Di Toro, G., and G. Pennacchioni (2005), Fault plane processes and mesoscopic structure of a strong-type seismogenic fault in tonalities (Adamello batholith, Southern Alps), *Tectonophys, 402*, 55-80.

Di Toro, G., G. Pennacchioni, and G. Teza, (2005), Can pseudotachylytes be used to infer earthquake source parameters? An example of limitations in the study of exhumed faults, *Tectonophys, 402*, 3-20.

Fossen, H. and J.Hesthammer (2000), Possible absence of small faults in the Gullfalks field, northern North Sea: Implications for downscaling faults in some porous sandstones. *J. Struct. Geol., 22, 851-863.*

Foxford, K. A., J. J. Walsh, J. Watterson, I. R. Garden, S. C. Guscott, and S. D. Burley (1998) Structure and content of the Moab Fault Zone, Utah, USA, and its implications for fault seal prediction. In: *Faulting, Fault Sealing and Fluid Flow in Hydrocarbon Reservoirs* edited by Jones, G., Fisher, Q. J. & Knipe, R. J. Geological Society, London, Special Publication 147, 87-103.

Hull, J. (1988), Thickness-displacement relationships for deformation zones, *J. Struct. Geol., 10*, 431-435.

Knott, S. D. (1994), Fault zone thickness versus displacement in the Permo-Triassic sandstones of NW England, *J. Geol. Soc., London, 151*, 17-25.

Knott, S. D., A. Beach, P. J. Brockbank, J. L. Brown, J. E. McCallum, and A. I. Welbon (1996), Spatial and mechanical controls on normal fault populations, *J. Struct. Geol., 18*, 359-372.

Little, T. A. (1995), Brittle deformation adjacent to the Awatere strike-slip fault in New Zealand: Faulting patterns, scaling relationships, and displacement partitioning, *Geol. Soc. Am. Bull., 107*, 1255-1271.

Marrett, R., and Allmendinger, R. W. (1990), Kinematic analysis of fault-slip data, *J. Struct. Geol., 12*, 973-986.

Otsuki, K. 1978. On the relationship between the width of shear zone and the displacement along fault. J. geol. Soc. Japan 84, 661-669.

Robertson, E. C. (1983), Relationship of fault displacement to gouge and breccia thickness, *American Institute of Mining Engineers Transactions*, *274*, 1426-1432.

Scholz, C. H. (1987), Wear and gouge formation in brittle faulting, *Geology, 15*, 493-495.

Segall, P., and D. D. Pollard (1983), Nucleation and Growth of Strike Slip Faults in Granite, *J. Geophys. Res., 88*, 555-568.

Seagall. P. & Simpson. C. 1986. Nucleation of ductile shear zones on dilatant fractures. Geology 14, 56-59.

Sibson, R. H (1975), Generation of pseudotachylyte by ancient seismic faulting, *Geophysical Journal of the Royal Astronomical Society, 43*, 775–794.